Inorganica Chimica Acta, *131* (1987) 45–52

Studies in Werner Clathrates.
Part 5*. Thermal Analysis of Bis(isothiocyanato)tetra(4-vinylpyridine)nickel(II) Inclusion Compounds. Crystal Structure of the $Ni(NCS)_2(4\text{-}Vipy)_4 \cdot 2CHCl_3$ Clathrate

MADELEINE H. MOORE, LUIGI R. NASSIMBENI** and MARGARET L. NIVEN

Department of Physical Chemistry, Unviersity of Cape Town, Rondebosch 7700, South Africa

(Received November 3, 1986)

Abstract

The clathrate structure $Ni(NCS)_2(4\text{-}Vipy)_4 \cdot 2CHCl_3$ has been elucidated. The $Ni(NCS)_2(4\text{-}Vipy)_4$ host molecule has an octahedral coordination and 'propeller' conformation. The $CHCl_3$ guest molecules occupy different cavities whose shapes and sizes are portrayed by volume calculations. Differential Thermal Analyses (DTA) and Gravimetric Thermal Analyses (GTA) were carried out on a series of clathrates comprising this host and a variety of guest molecules. An enthalpy change value for the 'guest release reaction' in each clathrate was obtained from the DTA experiments. The solubility of this host in these same guest solvents was measured in order to obtain a better understanding of the clathration process.

Introduction

There is a wide range of inclusion compounds called Werner Clathrates which have coordination compounds represented by the general formula MX_2B_4 as the host component. The majority of these compounds have been derived from the extensive experimental studies performed by Schaeffer *et al.* [2] (who first applied the 'clathrating ability' of MX_2B_4 complexes to mixture separation) and investigations by de Radzitzky and coworkers [3]. In the formula MX_2B_4, M is a divalent transition metal cation (e.g. Fe(II), Co(II), Ni(II), Cu(II), etc.), X denotes the anionic ligand (e.g. NCS^-, NCO^-, Br^-, etc.) and B is an electrically neutral substituted pyridine or α-arylalkylamine. The clathrating ability of a MX_2B_4 host complex depends on its molecular structure and, in particular, on the amine ligand (B) coordinated to M [4]. The most widely studied host complex is $Ni(NCS)_2(4\text{-}Mepy)_4$. Its clathrating ability is attributed to the remarkable rotational freedom of the pyridine rings about their Ni–N bonds [5] which enables the complex to adjust its molecular shape according to the size, shape and polarity of an incoming guest molecule. The sorption of guest molecules (typically aromatic hydrocarbons) has the ability to transform the non-clathrate α-phase $Ni(NCS)_2(4\text{-}Mepy)_4$ complex [6] into the porous tetragonal β-phase clathrate. The formation of inclusion compounds is stereoselective and may be used for the separation of isomer mixtures [7] and even isotopomers [8]. The physico-chemical behaviour of these clathrates, various crystal structures with different guest molecules and intermolecular host-guest interactions have been reviewed by Lipkowski [9].

We have synthesised and characterised the structures of: $Ni(NCS)_2(4\text{-}Mepy)_4 \cdot p\text{-}C_{10}H_{14}$, $Ni(NCS)_2(4\text{-}Mepy)_2(4\text{-}Phpy)_2 \cdot C_3H_8O_2$ [10], $Ni(NCS)_2(3\text{-}Mepy)_4 \cdot CHCl_3$, $Ni(NCS)_2(4\text{-}Phpy)_4 \cdot 4C_2H_6OS$ [11], $Ni(NCS)_2(4\text{-}Vipy)_4$ in its α-phase, and its β-phase clathrates with $p\text{-}C_8H_{10}$, $m\text{-}C_8H_{10}$ and $o\text{-}C_8H_{10}$ as guest molecules [12], and two structures of $Ni(NCS)_2(4\text{-}Etpy)_4$ in its non-porous α-phase and six structures of its clathrates with $p\text{-}C_8H_{10}$, $m\text{-}C_8H_{10}$, $o\text{-}C_8H_{10}$, CS_2 and CCl_4 as guest molecules [1]. We now report the γ-phase clathrate structure of $Ni(NCS)_2(4\text{-}Vipy)_4 \cdot 2CHCl_3$.

We carried out Differential Thermal Analysis (DTA) and Gravimetric Thermal Analysis (GTA) on a series of clathrates comprising the $Ni(NCS)_2(4\text{-}Vipy)_4$ host and a variety of guest molecules (*o*-xylene, *m*-xylene, $CHCl_3$ and THF).

A knowledge of the thermochemistry of enclathration reactions is pertinent to comprehend their physicochemical nature and has thus been the subject of calorimetric studies since 1962 [13]. In this work thermal analysis was used to study:

(a) The stoichiometry of the clathrates.

(b) The temperature at which guest molecules are released and the thermochemistry of this guest release reaction.

(c) The breakdown of the host complex.

A study of the solubility of this host complex in these solvents (*o*-xylene, *m*-xylene, $CHCl_3$ and THF) was carried out.

---

*For Part 4, see ref. 1.

**Author to whom correspondence should be addressed.

0020-1693/87/$3.50

Experimental

The host complex, Ni(NCS)$_2$(4-Vipy)$_4$, was prepared in powder form by reacting an aqueous solution of nickel isothiocyanate with a stoichiometric quantity of 4-vinylpyridine. The dried powder was dissolved in chloroform and layered with diethylether, to yield dark blue plate-shaped crystals which gradually crumbled to the host powder on exposure to air. The clathrate liberates the guest gradually under ambient conditions to leave a residual host metal complex, Ni(NCS)$_2$(4-Vipy)$_4$, as a fine powder.

The crystal densitiy was obtained using a linear density column containing water and KI solution in the range 1.00 to 1.40 g cm^{-3}. The column was calibrated with oil droplets of predetermined densities. The measurement was made in approximately five seconds hence this technique [14] was taken as the most accurate one for this unstable crystal.

Microanalysis was used to ascertain % C, % H and % N of compound **I**, the results are shown in Table I.

A single crystal of suitable size (0.25 X 0.37 X 0.50 mm) was wedged and sealed in a 0.5 mm Lindemann-glass capillary partly pre-filled with mother liquor at its tip portion.

The intensity data were collected at 294 K on a Nonius CAD4 diffractometer with graphite monochromated Mo Kα radiation ($\lambda = 0.7107$ Å). Lattice parameters were obtained from the angular settings of 25 centered reflections measured in the range $16° < \theta < 17°$. Scans were in the ω–2θ scan mode with a final acceptance limit of 20σ at 20° min^{-1} in ω and a maximum recording time of 40 s. The intensity variation of three standard reflections was monitored every hour to check crystal stability and recentering was carried out every 100 measured reflections. A Lorentz-polarization factor [15] was applied to the data but no correction was made for absorption. Crystal data and the experimental details of the intensity data collection are listed in Table I.

The structure was solved in $P2_1/n$ unique axis b (cell choice 2 with the origin at $\bar{1}$) by the heavy atom method and subsequent difference Fourier syntheses, with least-squares refinement of F magnitudes, using the SHELX76 [16] program system.

The final model employed anisotropic thermal parameters for the heavy atoms (Ni, S and Cl) and isotropic ones for all the others. The aromatic hydrogen atoms were subjected to constrained refinement, riding at 1.08 Å from their parent carbon atoms, with a common isotropic temperature factor. The two terminal H atoms on each vinyl group were placed in calculated positions (1.08 Å from the parent C atom) again with a single isotropic temperature factor. No H atoms were placed on the guest molecules. The maximum peak height in the final difference Fourier synthesis corresponds to less than 1 e Å^{-3}. Final refinement parameters are listed in Table I, and fractional atomic coordinates are given in Table II. Complex neutral atom scattering factors for hydrogen were taken from Stewart, Davidson and Simpson [17], and for all other atoms from Cromer and Mann [18], with dispersion corrections from Cromer and Liberman [19].

TABLE I. Crystal Data and Experimental and Refinement Parameters for Compound I

Crystal data	
Microanalysis C, H, N (%)	
determined	46.9, 3.6, 10.3
calculated	46.1, 3.6, 10.1
Molecular formula	$C_{32}H_{30}N_6NiS_2Cl_6$
Molecular weight (g mol^{-1})	832.44
Space group	$P2_1/n$
a (Å)	10.435(4)
b (Å)	19.787(6)
c (Å)	19.82(1)
β (°)	99.10(4)
V (Å^3)	40.2
Z	4
Host:guest ratio	1:2
D_m (g cm^{-3})	1.38
D_c (g cm^{-3})	1.37
μ (Mo Kα) (cm^{-1})	9.43
$F(000)$	1704
Data collection	
Scan width ($\Delta\omega$) (°)	$(0.85 + 0.35 \tan\theta)$
Aperture width (mm)	$(1.30 + 1.05 \tan\theta)$
Vertical aperture length (mm)	4
Range scanned (°)	$1 < \theta < 25$
Stability standard reflections (%)	1.87
No. reflections collected	7563
No. 'observed' reflections with $I_{rel} > 2\sigma I_{rel}$	3120
Final refinement	
Number of variables	261
$R = \Sigma\|\|F_o\| - \|F_c\|\|/\Sigma\|F_o\|$	0.0737
$R_w = \Sigma w^{1/2}\|\|F_o\| - \|F_c\|\|/\Sigma w^{1/2}\|F_o\|$	0.0694
Weighting scheme	$(\sigma^2 F)^{-1}$
U_{iso} (aromatic H) (Å^2)	0.136(3)
U_{iso} (vinyl H) (Å^2)	0.087(2)

Molecular parameters were obtained from the program PARST [20] and drawings from PLUTO [21]. All computations were carried out on a Sperry 1100 computer.

All thermograms were carried out on a Stanton–Redcroft Thermal Analyzer (model STA 780), operating at a uniform heating rate of 20 °C/min (starting at 40 °C and going to 400 °C). During each run nitrogen was passed through the cell at 87 ml/min. The sample container is a platinum crucible which sits directly on top of the thermocouple so that only

TABLE II. Fractional Atomic Coordinates ($\times 10^4$) and Thermal Parameters ($\times 10^3$) (with e.s.d.s in parentheses) of Compound I

Ni(1)	−83(1)	2517(1)	6706(1)	*					
N(1)	−1790(7)	3075(4)	6557(4)	68(2)	N(2)	1621(7)	1967(4)	6841(4)	71(2)
C(1)	−2668(9)	3424(5)	6525(4)	64(2)	C(2)	2614(8)	1705(4)	6878(4)	60(2)
S(1)	−3906(3)	3906(2)	6483(2)	*	S(2)	4009(2)	1337(1)	6921(2)	*
N(11)	1004(6)	3428(4)	6770(4)	61(2)	N(31)	−110(6)	2487(4)	5628(3)	65(2)
C(12)	2040(9)	3508(5)	6452(5)	73(2)	C(32)	237(9)	1938(5)	5315(5)	75(3)
C(13)	2655(9)	4112(5)	6414(5)	76(3)	C(33)	237(9)	1896(5)	4621(5)	82(3)
C(14)	2224(9)	4672(5)	6712(5)	79(3)	C(34)	−138(9)	2459(6)	4214(5)	80(2)
C(15)	1201(9)	4604(5)	7053(5)	76(3)	C(35)	−465(9)	3029(5)	4541(5)	81(3)
C(16)	597(9)	3979(5)	7070(5)	70(2)	C(36)	−458(9)	3030(5)	5235(5)	75(2)
C(17)	2790(11)	5390(6)	6678(6)	108(4)	C(37)	−181(10)	2475(7)	3468(6)	101(3)
C(18)	3638(16)	5520(8)	6321(8)	136(5)	C(38)	−10(16)	1953(10)	3096(10)	144(5)
N(21)	−100(7)	2529(4)	7772(3)	63(2)	N(41)	−1167(7)	1607(4)	6650(4)	64(2)
C(22)	−1188(9)	2479(5)	8041(5)	73(2)	C(42)	−777(9)	1075(5)	7046(5)	79(3)
C(23)	−1244(9)	2476(5)	8727(5)	77(2)	C(43)	−1477(10)	485(6)	7024(6)	90(3)
C(24)	−110(10)	2501(5)	9170(5)	86(3)	C(44)	−2582(11)	445(6)	6598(6)	92(3)
C(25)	1055(9)	2537(5)	8920(5)	78(2)	C(45)	−3036(11)	975(6)	6182(6)	102(3)
C(26)	1004(9)	2553(5)	8227(5)	71(2)	C(46)	−2294(10)	1559(5)	6225(5)	85(3)
C(27)	4(12)	2481(7)	9970(7)	121(4)	C(47)	−3598(19)	−216(9)	6439(10)	174(6)
C(28)	−977(16)	2652(8)	10252(9)	151(5)	C(48)	−3279(23)	−711(12)	6701(13)	224(9)
CG(1)	7406(11)	334(6)	9097(6)	98(3)	CG(2)	7580(12)	46(6)	4043(7)	123(4)
Cl(11)	8556(4)	812(2)	9620(2)	*	Cl(21)	7398(5)	−346(3)	4823(2)	*
Cl(12)	6634(4)	829(2)	8429(2)	*	Cl(22)	7136(4)	852(2)	4075(3)	*
Cl(13)	6250(4)	53(2)	9586(2)	*	Cl(23)	9130(5)	−54(2)	3926(3)	*

*Anisotropic atoms have thermal parameters of the form:
$T = \exp\{-2\pi^2(U_{11}h^2a^{*2} + U_{22}k^2b^{*2} + U_{33}l^2c^{*2} + 2U_{23}klb^*c^* + 2U_{13}hla^*c^* + 2U_{12}hka^*b^*) \times 10^3\}$
with parameters:

	U_{11}	U_{22}	U_{33}	U_{23}	U_{13}	U_{12}
Ni(1)	56(1)	48(1)	76(1)	2(1)	11(1)	5(1)
S(1)	81(2)	92(2)	209(4)	19(2)	27(2)	31(1)
S(2)	71(1)	84(1)	100(2)	−1(1)	15(1)	23(1)
Cl(11)	168(3)	158(3)	156(3)	−8(2)	22(2)	−60(2)
Cl(12)	189(3)	145(3)	126(3)	9(2)	28(2)	−10(2)
Cl(13)	182(3)	179(4)	153(3)	11(3)	59(3)	−58(3)
Cl(21)	278(5)	195(4)	157(4)	8(3)	49(3)	49(4)
Cl(22)	187(4)	97(3)	302(6)	−20(3)	−10(9)	26(2)
Cl(23)	216(4)	125(3)	401(8)	−27(4)	146(5)	10(3)

the furnace temperature can be measured directly. The lag between this and the sample temperature was estimated using a standard indium sample ($T_{\mathrm{melt}} = 157$ °C).

Discussion

The host nickel complex in compound **I** crystallises as discrete mononuclear molecules with each nickel atom coordinated to six nitrogen donor ligands in such a way that they form an irregular octahedron with the two isothiocyanate moieties *trans* to each other. A perspective view of a host molecule is shown in Fig. 1. The torsional configuration of the 4-vinyl pyridine ligands is given by the torsion angles: N(1)–Ni(1)–N(x1)–C(x2) with $x = 1$ ($\tau 1$), 2 ($\tau 2$), 3 ($\tau 3$) and 4 ($\tau 4$), which have the following values: $\tau 1 = -136.0°$ (44.0°), $\tau 2 = 37.6°$, $\tau 3 = -141.1°$ (38.9°) and $\tau 4 = -142.5°$ (37.5°). The values in brackets are obtained by neglecting the asymmetry of the pyridine ring. This conformation is then indicative of a ++++ 'propeller' commonly found in complexes of this type [12, 22].

The two crystallographically-independent chloroform guest molecules were located in two different channels; their location is shown in Fig. 2. Volume calculations using the program OPEC [23] were employed to determine the exact size and shape of the channels. Their topology is depicted in Fig. 3, which displays 2.2 unit cells sectioned at $y = 0$, where the channels are at their widest. Both channels are wide enough (maximum widths are 11.7 Å, channel 1, and 12.0 Å, channel 2) to accommodate two guest

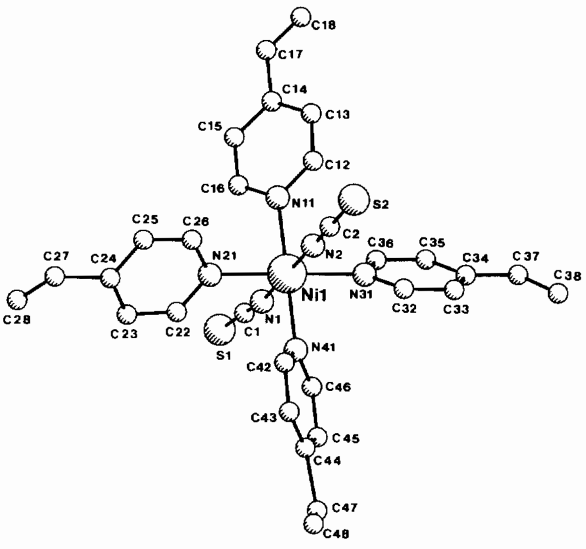

Fig. 1. Perspective view of a host molecule of compound I with atomic nomenclature.

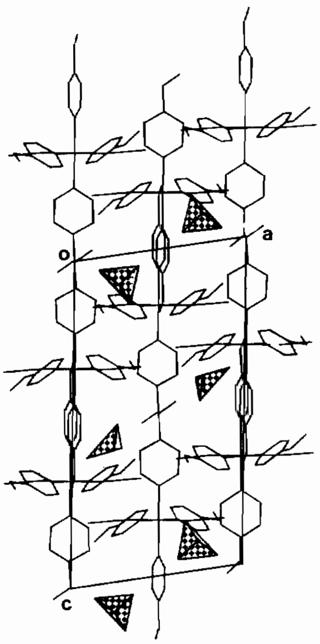

Fig. 2. Projection of the γ-phase clathrate (compound I) down b.

molecules related to each other by an inversion centre, Wyckoff positions d (channel 1) and b (channel 2). The volume available to these two guest molecules was calculated to be approximately 171 Å^3 (channel 1) and 223 Å^3 (channel 2); the volume an ordered chloroform molecule occupies is 68 Å^3 according to Kitaigorodski [24]. As expected the anisotropy of the guest molecule occupying the larger channel is more pronounced than that of the other guest molecule (Table II).

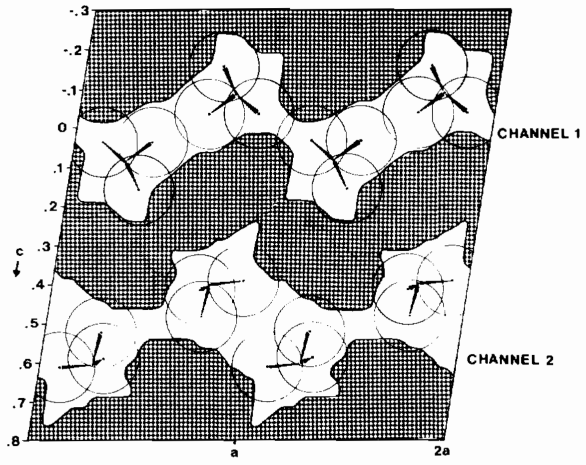

Fig. 3. The topologies of the two different channels sectioned at $y = 0$.

The thermal analysis results are shown in Fig. 4 and are summarised in Table III. Bond lengths of compound I are given in Table IV, bond angles in Table V and selected torsion angles in Table VI.

The GTA curves show that the mechanism of decomposition is invariably

$$\begin{array}{l} \mathrm{NiX_2B_4 \cdot nG(s)} \\ \quad\downarrow \\ \mathrm{NiX_2B_4(s) + nG(g)} \\ \quad\downarrow \\ \mathrm{NiX_2B_2(s) + 2B(g)} \\ \quad\downarrow \\ \mathrm{NiX_2(s) + 2B(g)} \end{array}$$

where: $X = NCS^-$, B = 4-Vipy.

The percentage weight loss, as reported in Table III, shows that there is excellent agreement between experimental and theoretical values, which never differ by more than 2%.

The DTA experiments were used to evaluate the enthalpy of the 'guest-release reaction'. This was established by measuring the area under the first endotherm in each DTA run. This area was assumed to be proportional to the enthalpy change, ΔH, in the following way: $\Delta H = A \times k/m$, where m = the sample mass (g), A = the area (cm^2) and k = the calibration factor. The calibration factor, k, was obtained by relating the melting of the pure metal indium standard ($\Delta H_{\mathrm{melt}} = 28.5$ J/g) to the measured peak area of this enthalpy change. It is interesting to note the different temperatures at which the guests are released, *viz.*

1.8THF <	2CHCl$_3$ <	0.25 4-Vipy <	1 *o*-xylene <	1 *p*-xylene
47 °C	62 °C	90 °C	102 °C	125 °C

This corresponds to our experiences in handling the single crystals of these clathrates for structural

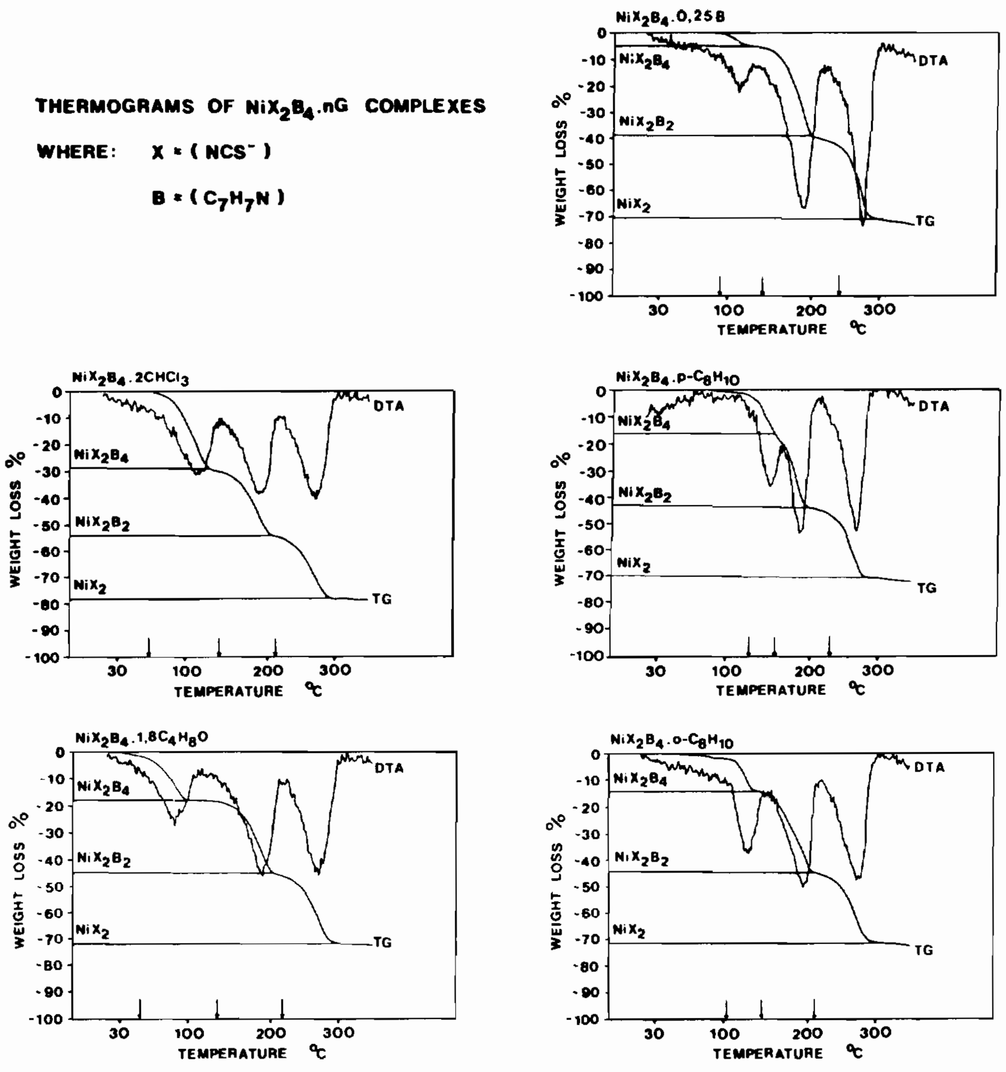

Fig. 4. Thermograms (TGA and DTA) of the clathrates of $Ni(NCS)_2(4\text{-}Vipy)_4$ with various guest molecules.

analyses. The THF clathrate is so unstable that we never managed to isolate and mount a single crystal and the $CHCl_3$ clathrate is visibly more unstable than the corresponding xylene compounds.

The temperature of the ‘guest release reaction’ of *p*-xylene is higher than that of *o*-xylene. This accords with results obtained from crystal structure analyses [12] which showed that the *p*-xylene structure is more efficiently packed.

When the different guest molecules are released they cause different amounts of damage to their respective host structures. This is illustrated by the variation in values obtained for the areas under the DTA curves for the decomposition of the host complex in its different clathrates.

In order to obtain a better understanding of the clathration process we measured the solubility of this host complex, $Ni(NCS)_2(4\text{-}Vipy)_4$, in the

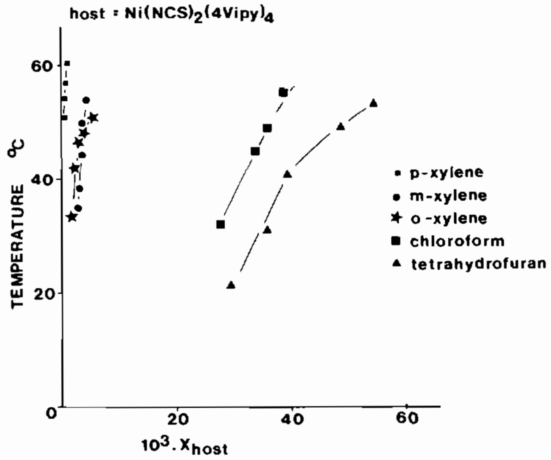

Fig. 5. Solubility curves of the $Ni(NCS)_2(4\text{-}Vipy)_4$ complex in the various guest solvents.

TABLE III. Thermal Analyses Results

	Calculated weight loss (%)	Measured weight loss (%)	Sample temperature (°C)	Area (cm^2)	ΔH (J/g)	ΔH (kJ/mol)
NiX_2B_4[a]$\cdot 0.25B \rightarrow NiX_2B_4 + 0.25B$	4.2	4.5	90	3.8	70	44
$NiX_2B_4 \rightarrow NiX_2B_2 + 2B$	38.1	39.0	140	14.9	276	164
$NiX_2B_2 \rightarrow NiX_2 + 2B$	71.8	70.0	243	12.3	228	124
$NiX_2B_4\cdot o\text{-}C_8H_{10} \rightarrow NiX_2B_4 + o\text{-}C_8H_{10}$	15.1	14.6	102	6.2	115	81
$NiX_2B_4 \rightarrow NiX_2B_2 + 2B$	45.0	44.6	141	10.2	189	113
$NiX_2B_2 \rightarrow NiX_2 + 2B$	75.0	70.8	207	9.5	176	96
$NiX_2B_4\cdot p\text{-}C_8H_{10} \rightarrow NiX_2B_4 + p\text{-}C_8H_{10}$	15.1	16.1	125	5.7	105	74
$NiX_2B_4 \rightarrow NiX_2B_2 + 2B$	45.0	42.7	155	7.5	139	83
$NiX_2B_2 \rightarrow NiX_2 + 2B$	75.0	70.0	228	7.5	139	75
$NiX_2B_4\cdot 2CHCl_3 \rightarrow NiX_2B_4 + 2CHCl_3$	28.6	28.8	62	9.6	178	102
$NiX_2B_4 \rightarrow NiX_2B_2 + 2B$	53.8	54.6	140	8.9	165	98
$NiX_2B_2 \rightarrow NiX_2 + 2B$	79.0	77.7	209	8.2	152	83
$NiX_2B_4\cdot 1.8C_4H_8O \rightarrow NiX_2B_4 + 1.8C_4H_8O$	18.0	18.0	47	6.5	120	87
$NiX_2B_4 \rightarrow NiX_2B_2 + 2B$	46.9	45.0	154	11.5	213	127
$NiX_2B_2 \rightarrow NiX_2 + 2B$	75.9	72.5	218	9.6	178	97

[a] $NiX_2B_4 = Ni(NCS)_2(4\text{-}Vipy)_4$

TABLE IV. Bond Lengths (Å) of Compound I (with e.s.d.s in parentheses)

Ni(1)–N(1)	2.077(7)	Ni(1)–N(2)	2.066(7)	Ni(1)–N(31)	2.133(6)
Ni(1)–N(11)	2.123(7)	Ni(1)–N(21)	2.116(6)	Ni(1)–N(41)	2.120(8)
S(1)–C(1)	1.597(10)	S(2)–C(2)	1.617(8)	N(1)–C(1)	1.141(12)
N(2)–C(2)	1.151(11)	N(31)–C(36)	1.343(12)	N(31)–C(32)	1.329(12)
C(36)–C(35)	1.374(14)	C(35)–C(34)	1.371(15)	C(33)–C(34)	1.395(14)
C(34)–C(37)	1.473(15)	C(33)–C(32)	1.378(14)	C(37)–C(38)	1.298(24)
N(11)–C(12)	1.344(12)	N(11)–C(16)	1.343(12)	C(12)–C(13)	1.364(13)
C(13)–C(14)	1.365(14)	C(14)–C(15)	1.357(14)	C(14)–C(17)	1.544(15)
C(15)–C(16)	1.391(13)	C(17)–C(18)	1.244(21)	N(21)–C(26)	1.347(10)
N(21)–C(22)	1.332(12)	C(26)–C(25)	1.367(14)	C(25)–C(24)	1.385(14)
C(24)–C(23)	1.358(13)	C(24)–C(27)	1.572(17)	C(23)–C(22)	1.370(14)
C(27)–C(28)	1.287(22)	N(41)–C(46)	1.337(11)	N(41)–C(42)	1.337(12)
C(46)–C(45)	1.386(15)	C(45)–C(44)	1.371(16)	C(44)–C(43)	1.319(14)
C(44)–C(47)	1.682(21)	C(43)–C(42)	1.374(15)	C(47)–C(48)	1.134(29)
CG(1)–Cl(11)	1.735(11)	CG(1)–Cl(12)	1.739(11)	CG(1)–Cl(13)	1.753(11)
CG(2)–Cl(21)	1.767(13)	CG(2)–Cl(22)	1.666(13)	CG(2)–Cl(23)	1.681(12)

TABLE V. Bond Angles (°) of Compound I (with e.s.d.s in parentheses)

N(31)–Ni(1)–N(11)	90.3(0.3)	N(31)–Ni(1)–N(21)	178.5(0.3)	N(31)–Ni(1)–N(41)	90.1(0.3)
N(11)–Ni(1)–N(21)	91.1(0.2)	N(11)–Ni(1)–N(41)	179.6(0.3)	N(21)–Ni(1)–N(41)	88.5(0.3)
N(1)–Ni(1)–N(2)	179.2(0.3)	N(1)–Ni(1)–N(31)	89.8(0.3)	N(1)–Ni(1)–N(11)	89.7(0.3)
N(1)–Ni(1)–N(21)	89.6(0.3)	N(1)–Ni(1)–N(41)	90.3(0.3)	N(2)–Ni(1)–N(31)	89.4(0.3)
N(2)–Ni(1)–N(11)	89.9(0.3)	N(2)–Ni(1)–N(21)	91.1(0.3)	N(2)–Ni(1)–N(41)	90.0(0.3)
N(1)–C(1)–S(1)	179.4(0.9)	N(2)–C(2)–S(2)	179.4(0.8)	Ni(1)–N(1)–C(1)	173.1(0.7)
Ni(1)–N(2)–C(2)	179.4(0.8)	Ni(1)–N(31)–C(36)	121.2(0.5)	Ni(1)–N(31)–C(32)	121.9(0.5)
Ni(1)–N(11)–C(12)	122.3(0.6)	Ni(1)–N(11)–C(16)	120.8(0.6)	Ni(1)–N(21)–C(26)	121.9(0.5)
Ni(1)–N(21)–C(22)	122.8(0.5)	Ni(1)–N(41)–C(46)	120.1(0.6)	Ni(1)–N(41)–C(42)	121.8(0.6)
C(36)–N(31)–C(32)	116.9(0.7)	N(31)–C(36)–C(35)	122.5(0.8)	C(36)–C(35)–C(34)	120.8(0.9)
C(35)–C(34)–C(33)	116.9(0.9)	C(35)–C(34)–C(37)	119.1(0.9)	C(33)–C(34)–C(37)	124.0(0.9)
C(34)–C(33)–C(32)	119.0(0.9)	C(33)–C(32)–N(31)	123.9(0.8)	C(34)–C(37)–C(38)	124.6(1.3)
C(12)–N(11)–C(16)	116.5(0.6)	N(11)–C(12)–C(13)	123.3(0.9)	C(12)–C(13)–C(14)	119.8(0.9)

(continued)

TABLE V. *(continued)*

C(13)–C(14)–C(15)	118.3(0.9)	C(13)–C(14)–C(17)	125.0(0.9)	C(15)–C(14)–C(17)	116.7(0.9)
C(14)–C(15)–C(16)	119.6(0.9)	C(15)–C(16)–N(11)	122.4(0.8)	C(14)–C(17)–C(18)	121.8(1.1)
C(26)–N(21)–C(22)	115.3(0.7)	N(21)–C(26)–C(25)	124.4(0.8)	C(26)–C(25)–C(24)	117.6(0.9)
C(25)–C(24)–C(23)	119.6(0.9)	C(25)–C(24)–C(27)	115.6(0.9)	C(23)–C(24)–C(27)	124.8(0.9)
C(24)–C(23)–C(22)	118.2(0.9)	C(23)–C(22)–N(21)	124.8(0.8)	C(24)–C(27)–C(28)	119.6(1.2)
C(46)–N(41)–C(42)	118.0(0.8)	N(41)–C(46)–C(45)	121.7(0.9)	C(46)–C(45)–C(44)	117.7(0.9)
C(45)–C(44)–C(43)	121.5(0.9)	C(45)–C(44)–C(47)	109.5(1.0)	C(43)–C(44)–C(47)	128.9(1.1)
C(44)–C(43)–C(42)	118.5(1.0)	C(43)–C(42)–N(41)	122.6(0.9)	C(44)–C(47)–C(48)	117.1(1.8)
Cl(12)–CG(1)–Cl(11)	110.0(0.7)	Cl(13)–CG(1)–Cl(11)	108.3(0.6)	Cl(13)–CG(1)–Cl(12)	108.8(0.6)
Cl(22)–CG(2)–Cl(21)	108.5(0.8)	Cl(23)–CG(2)–Cl(21)	107.9(0.8)	Cl(23)–CG(2)–Cl(22)	113.5(0.8)

TABLE VI. Selected Torsion Angles (°) of Compound I (with e.s.d.s in parentheses)

N(1)–Ni(1)–N(31)–C(36)	40.2(0.7)	N(2)–Ni(1)–N(31)–C(36)	–139.5(0.7)
N(1)–Ni(1)–N(31)–C(32)	–141.1(0.7)	N(2)–Ni(1)–N(31)–C(32)	39.3(0.7)
N(1)–Ni(1)–N(11)–C(12)	–136.0(0.7)	N(2)–Ni(1)–N(11)–C(12)	43.2(0.7)
N(1)–Ni(1)–N(11)–C(16)	36.5(0.7)	N(2)–Ni(1)–N(11)–C(16)	–144.3(0.7)
N(1)–Ni(1)–N(21)–C(26)	–145.9(0.7)	N(2)–Ni(1)–N(21)–C(26)	33.8(0.7)
N(1)–Ni(1)–N(21)–C(22)	37.6(0.7)	N(2)–Ni(1)–N(21)–C(22)	–142.7(0.7)
N(1)–Ni(1)–N(41)–C(46)	35.5(0.7)	N(2)–Ni(1)–N(41)–C(46)	–143.7(0.7)
N(1)–Ni(1)–N(41)–C(42)	–142.5(0.7)	N(2)–Ni(1)–N(41)–C(42)	38.3(0.7)
N(31)–Ni(1)–N(11)–C(12)	–46.2(0.7)	N(31)–Ni(1)–N(11)–C(16)	126.3(0.7)
N(31)–Ni(1)–N(41)–C(46)	–54.3(0.7)	N(31)–Ni(1)–N(41)–C(42)	127.7(0.7)
N(11)–Ni(1)–N(21)–C(26)	–56.2(0.7)	N(11)–Ni(1)–N(21)–C(22)	127.3(0.7)
N(11)–Ni(1)–N(31)–C(36)	–49.6(0.7)	N(11)–Ni(1)–N(31)–C(32)	129.2(0.7)
N(21)–Ni(1)–N(41)–C(46)	125.2(0.7)	N(21)–Ni(1)–N(41)–C(42)	–52.8(0.7)
N(21)–Ni(1)–N(11)–C(12)	134.3(0.7)	N(21)–Ni(1)–N(11)–C(16)	–53.2(0.7)
N(41)–Ni(1)–N(31)–C(36)	130.5(0.7)	N(41)–Ni(1)–N(31)–C(32)	–50.8(0.7)
N(41)–Ni(1)–N(21)–C(26)	123.8(0.7)	N(41)–Ni(1)–N(21)–C(22)	–52.7(0.7)

various guest solvents. The results are shown in Fig. 5 which depicts the mole fraction of host complex which is soluble at various temperatures. The host complex is notably less soluble in the xylenes (in particular *p*-xylene), which, however, are the guests that yield more stable crystalline clathrates (the most stable being with *p*-xylene as the guest). This can be understood in terms of simple thermodynamic considerations.

The equilibrium constant for the reaction

$$\mathrm{H(solution)} + n\mathrm{G(1)} = \mathrm{HG}_n\mathrm{(s)}$$

where H = host complex, G = guest solvent

is approximated by

$$K = [\mathrm{HG}_n]/[\mathrm{H}]\,[\mathrm{G}]^n$$

since the clathrate is a solid, and the guest concentration is in great excess (therefore effectively constant), the equilibrium constant, K, is inversely proportional to the host complex concentration in solution (*i.e.*, $K \propto 1/[\mathrm{H}]$). Thus the less soluble the host complex is in a given guest solvent, the higher the value of K, and hence the solid clathrate is more readily formed.

References

1 M. H. Moore, L. R. Nassimbeni and M. L. Niven, *J. Chem. Soc., Dalton Trans.*, in publication.

2 W. D. Schaeffer, W. S. Dorsey, D. A. Skinner and J. Christian, *J. Am. Chem. Soc.*, *79*, 5870 (1957).

3 P. de Radzitzky and J. Hanotier, *Ind. Eng. Chem. Process Des. Dev.*, *1*, 10 (1962).

4 J. Hanotier and P. de Radzitzky, in J. L. Atwood, J. E. D. Davies and D. D. MacNicol (eds.), 'Inclusion Compounds', Vol. 1, Academic Press, London, 1984, Chap. 4.

5 J. Lipkowski, 'Structure and Physico-Chemical Behaviour of Clathrates formed of the $Ni(NCS)_2(4\text{-methylpyridine})_4$ Complex', Polskiej Akademii Nauk, Wroclaw/Warsaw/Krakow/Gdansk, 1980.

6 S. A. Allison and R. M. Barrer, *J. Chem. Soc. A*, 1717 (1969).

7 P. Starzewski and J. Lipkowski, *Pol. J. Chem.*, *53*, 1869 (1979).

8 S. E. Ofodile, R. M. Kellett and N. O. Smith, *J. Am. Chem. Soc.*, *101*, 7725 (1979).

9 J. Lipkowski, in J. L. Atwood, J. E. D. Davis and D. D. MacNicol (eds.), 'Inclusion Compounds', Vol. 1, Academic Press, London, 1984, Chap. 3.

10 D. R. Bond, G. E. Jackson and L. R. Nassimbeni, *S. Afr. J. Chem.*, *36*, 19 (1983).

11 L. R. Nassimbeni, S. Papanicolaou and M. H. Moore, *J. Incl. Phenom.*, *4*, 31 (1986).

12 M. H. Moore, L. R. Nassimbeni, M. L. Niven and M. W. Taylor, *Inorg. Chim. Acta, 115*, 211 (1986).

13 H. J. Hart and N. O. Smith, *J. Am. Chem. Soc., 101*, 7725 (1979).

14 G. Oster and M. Yamamoto, *Chem. Rev., 63*, 257 (1963).

15 J. S. Kasper and K. Lonsdale (eds.), 'International Tables for X-ray Crystallography', Vol. II, Kynoch Press, Birmingham, p. 266.

16 G. M. Sheldrick, 'SHELX-76 program system', in H. Schenk, R. Olthof-Hazekamp, H. van Koningsvelt and G. C. Bassi (eds.), 'Computing in Crystallography', Delft University Press, 1978, p. 34.

17 R. F. Stewart, E. R. Davidson and W. T. Simpson, *J. Chem. Phys., 42*, 3175 (1965).

18 D. T. Cromer and J. B. Mann, *Acta Crystallogr., Sect. A, 24*, 321 (1968).

19 D. T. Cromer and D. Liberman, *J. Chem. Phys., 53*, 1891 (1970).

20 M. Nardelli, *Comput. Chem., 7*, 95 (1983).

21 W. D. S. Motherwell, 'PLUTO Plotting Program', Cambridge University, U.K., unpublished.

22 J. Lipkowski, *J. Mol. Struct., 75*, 13 (1981).

23 A. Gavezzotti, OPEC Organic Packing Energy Calculations Program, *J. Am. Chem. Soc., 105*, 5220 (1983).

24 A. I. Kitaigorodski, 'Molecular Crystals and Molecules', Academic Press, New York, 1973, Chap. 1.